

RESEARCH ARTICLE | FEBRUARY 14 2023

Decomposition of mechanical stress effect on the magnetic property of silicon steel sheet

Special Collection: [67th Annual Conference on Magnetism and Magnetic Materials](#)H. Shimizu; Y. Marumo; Y. Mishima; T. Matsuo  

Check for updates

AIP Advances 13, 025151 (2023)

<https://doi.org/10.1063/9.0000450>View
OnlineExport
Citation

26 August 2024 04:26:04

AIP AdvancesSpecial Topic: Novel Applications of
Focused Ion Beams — Beyond Milling**Submit Today**

Decomposition of mechanical stress effect on the magnetic property of silicon steel sheet

Cite as: AIP Advances 13, 025151 (2023); doi: 10.1063/9.0000450

Submitted: 3 October 2022 • Accepted: 28 January 2023 •

Published Online: 14 February 2023



H. Shimizu, Y. Marumo, Y. Mishima, and T. Matsuo^{a)}

AFFILIATIONS

Kyoto University, Kyoto 615-8510, Japan

Note: This paper was presented at the 67th Annual Conference on Magnetism and Magnetic Materials.

^{a)}Author to whom correspondence should be addressed: matsuo.tetsuji.5u@kyoto-u.ac.jp

ABSTRACT

A principal stress decomposition method was examined and compared with the equivalent stress theory to evaluate the stress-dependent magnetic properties of nonoriented silicon steel. A physical magnetization model, the multidomain particle model, was used to simulate the stress dependence of the magnetic properties by applying mechanical stress in different directions relative to the magnetic field direction. Experimental and computational tests show that even though the principal stress decomposition method provides a reasonable evaluation of the stress-dependent properties in the stress direction, it fails to accurately predict the properties in the perpendicular direction. To improve the prediction accuracy, a modified decomposition method is proposed, which gives a reasonable evaluation of the stress dependence of BH loops, permeability and hysteresis loss even when the magnetization direction is different from the stress direction.

© 2023 Author(s). All article content, except where otherwise noted, is licensed under a Creative Commons Attribution (CC BY) license (<http://creativecommons.org/licenses/by/4.0/>). <https://doi.org/10.1063/9.0000450>

I. INTRODUCTION

Experimental and computational studies on the stress-dependent magnetic properties of iron-core materials are ongoing. Generally, the direction of applied stress differs from the magnetization direction. However, conducting measurements under all vector/tensor combinations of the magnetization and stress directions is impractical. Several stress models^{1–3} have been proposed to avoid such measurements under arbitrary combinations of stress and magnetization directions. For example, the equivalent stress theory has been experimentally validated^{2,3} and has been applied to motor analysis.⁴ Another solution is to use a physical magnetization model that can computationally predict stress-dependent magnetic properties without using measured data under mechanical stress.

A physical magnetization model, an energy-based multi-scale magnetization model called “multidomain particle model” (MDPM),⁵ was recently developed. The MDPM can effectively predict the stress-dependent loss properties of silicon steel without measuring the stress-dependent properties.

Equivalent stress theory aims to estimate the stress-dependent magnetic properties in the excitation direction. In this study, another stress model was examined to extend the applicable direction of

stress theory: the principal stress decomposition method,¹ which has not yet been tested experimentally and computationally. We compare it with the equivalent stress theory using the MDPM under mechanical stress, the direction of which is different from that of the magnetic field.

II. MDPM

The MDPM⁵ is a physical macroscopic magnetization model developed by assembling mesoscopic particles at the crystal-grain scale, called “simplified domain structure models” (SDSMs) (Fig. 1).

The magnetization state of each particle is determined to determine the local minimum of the total magnetic energy, which comprises the Zeeman, crystalline anisotropy, magnetostatic, and magnetoelastic energies. A pinning field is generated in every particle representing the domain-wall motion, which is modeled by the play model. The pinning field distribution is estimated based on the measured BH (magnetization) loops under the stress-free condition, whereas the other model parameters were obtained from the material constants: the spontaneous magnetization, anisotropy, and magnetostriction constants.

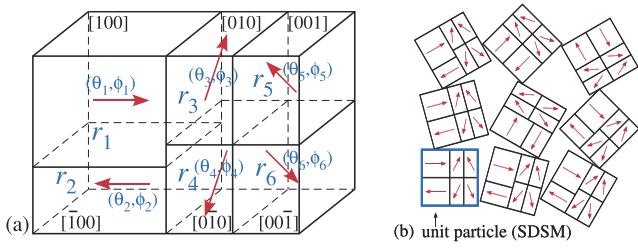


FIG. 1. MDPM: (a) mesoscopic six-domain particle (SDSM) and (b) MDPM comprising an assembly of multi-domain particles.

III. STRESS MODELS

This section discusses the effect of in-plane stress $\sigma = \text{diag}(\sigma_x, \sigma_y, 0)$ where the x - and y -directions are the principal directions. The direction of the applied magnetic field is given by a unit vector $\mathbf{h} = (h_x, h_y, 0)$.

A. Equivalent stress model

According to a simple version of the equivalent stress theory,² the effect of σ along \mathbf{h} is evaluated as an equivalent stress σ_{eq} as

$$\sigma_{eq} = (\sigma_x - \sigma_y/2)h_x^2 + (\sigma_y - \sigma_x/2)h_y^2. \quad (1)$$

When $\sigma_y = 0$ and $\mathbf{h} = (1, 1, 0)/\sqrt{2}$, then $\sigma_{eq} = \sigma_x/4$. A more detailed version³ has also been developed. Both models successfully estimate the stress effects along the magnetization direction.

B. Principal stress decomposition method

The separation of the stress effect in the principal stress directions has been proposed in Ref. 1. It assumes that the stress effect and magnetization property along one principal direction are independent of those along the other principal direction, which can be expressed as follows.

$$B_x = f_x(H_x, \sigma_x), \quad B_y = f_y(H_y, \sigma_y) \quad (2)$$

The assumption mentioned above is not realistic primarily because the magnetic property in the y -direction is not independent of H_x and B_x and depends on the stress applied in the x -direction. Moreover, the compressive stress in the x -direction generally works as a tensile stress in the y -direction according to the equivalent stress theory. However, the effect of tensile stress is not as large as that of compressive stress. In addition, according to experimental results, when B is small, the magnetic properties in one direction are approximately independent of those in the perpendicular direction and can facilitate a reasonable estimation of the stress effect. The inadequacy of the above assumption and its remedy are discussed in Sec. V.

IV. EXPERIMENTAL TESTS

The stress-dependent magnetic properties were measured at 50 Hz using a rotational single-sheet tester (RSST)⁶ to evaluate the equivalent stress theory and principal stress decomposition method. The measurement setup is shown in Fig. 2. The tester can apply

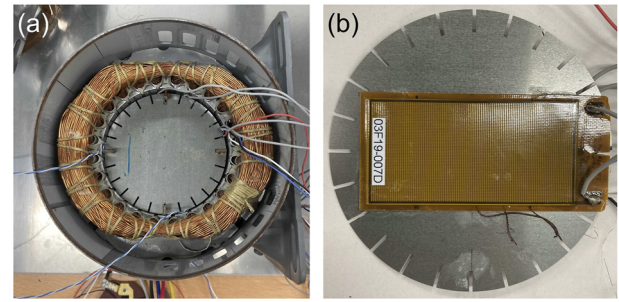


FIG. 2. RSST: (a) Top view of the rotational single-sheet tester (b) NO steel sheet with piezoelectric films.

a magnetic flux to the silicon steel sheet in any direction. The B- and H-vectors are detected by the pickup coils. Compressive stress can be applied along the rolling direction (RD) by attaching piezoelectric films on both sides of the sample sheet. The magnitude of the applied stress is estimated from the strain measured by strain gauges.

A non-oriented (NO) steel sheet, JIS:35A300, was measured and simulated in this study. The direction of the uniaxial stress is denoted by φ_σ , the direction of the applied magnetic field is denoted by φ_H , and RD denotes the x -direction. The stress dependence of the iron loss w , was measured using the RSST. The difference Δw in the iron loss from the stress-free condition is discussed hereafter. Compressive stress was applied along $\varphi_\sigma = 0$, and the magnetic field was applied along $\varphi_H = 0, \pi/6$, and $\pi/4$.

A. Equivalent stress theory

According to the equivalent stress theory defined by (1), if a magnetic field is applied along $\varphi_H = \pi/4$ and compressive stress is applied along $\varphi_\sigma = 0$, then the magnetic property is equal to that under the equivalent compressive stress $\sigma_{eq} = \sigma_x/4$ along $\varphi_\sigma = \pi/4$. Similarly, the equivalent stress along $\varphi_H = \pi/6$ is $\sigma_{eq} = 5\sigma_x/8$. However, in this measurement setup, compressive stress can only be applied along the RD. Instead of applying stress in the $\pi/4$ and $\pi/6$ directions, the stress dependence when $\varphi_H = \varphi_\sigma = 0$ is compared with that when $\varphi_H = \pi/4, \pi/6$, and $\pi/4$.

Figure 3(a) compares Δw when the magnetic field is in the direction of $\varphi_H = 0, \pi/6$, and $\pi/4$ when the amplitude of B is 1.2 T. The effect of stress decreases with an increase in φ_H as predicted by the equivalent stress theory. In Fig. 3(b), the horizontal axis was replaced by the equivalent stress to consider the angle between φ_σ and φ_H , which shows that the equivalent stress theory estimates the property along $\varphi_H = \pi/6$ based on that along $\varphi_H = \varphi_\sigma = 0$.

However, the estimated stress dependence differs from the measured result when $\varphi_H = \pi/4$. In particular, the iron loss decreases even with an increase in compressive stress when $\varphi_H = \pi/4$ and the stress is small. This is mainly attributed to the anisotropy of the steel sheet. The iron loss w is decomposed into $w_x = \int H_x dB_x$ and $w_y = \int H_y dB_y$. The loss w_x increases with the stress along the RD, whereas w_y decreases because σ_x acts as a tensile stress along the transverse direction (TD) according to the equivalent stress theory.

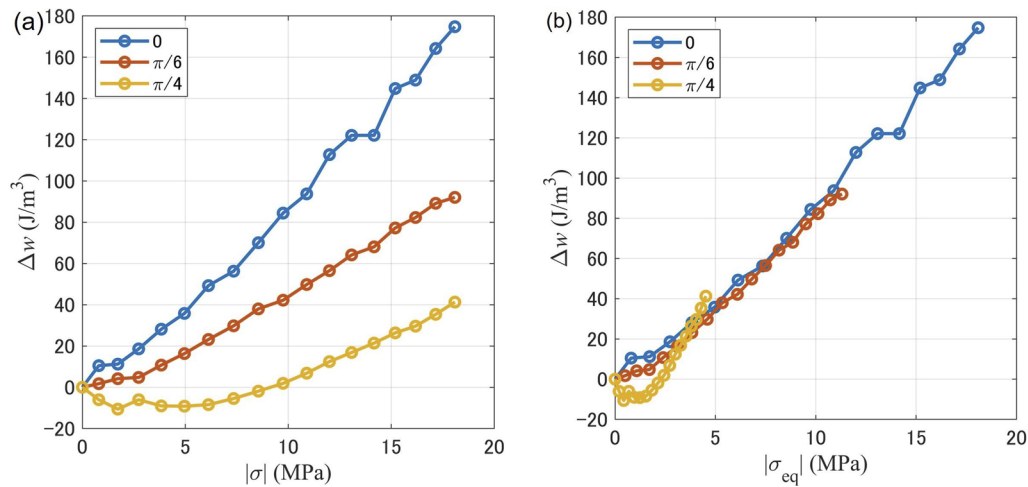


FIG. 3. σ - Δw property along $\varphi_H = 0, \pi/6, \pi/4$ at $B = 1.2$ T: (a) dependence on stress $|\sigma|$ and (b) dependence on equivalent stress $|\sigma_{eq}|$.

Owing to the anisotropy, the decrement in w_y exceeds the increment in w_x . Admittedly, the equivalent stress theory can predict the decrease in w_y ; however, it fails to evaluate the decrease in the total loss w because it does not fully consider the anisotropy of the steel sheet.

In contrast, when $\varphi_H = \pi/6$, the iron loss increases monotonically with stress, suggesting that the estimation of magnetization properties based on the equivalent stress theory is accurate if the magnetization direction is near to the stress direction and the influence of the perpendicular direction is small.

Therefore, a decomposed description based on the stress direction is necessary to consider the anisotropy of the material.

B. Principal stress decomposition method

In this study, Δw was decomposed into Δw_x (RD) and Δw_y (TD) to evaluate the principal stress decomposition method.

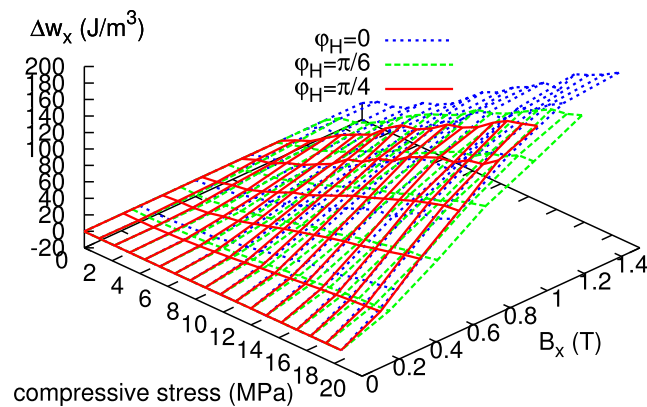


FIG. 4. Comparison of Δw_x when $\varphi_H = 0, \pi/6$, and $\pi/4$.

Figure 4 compares the decomposed component Δw_x under excitation angles $\varphi_H = 0, \pi/6$, and $\pi/4$. The influence of B_y on the iron loss Δw_x is small, regardless of the amplitude of B_x , suggesting that the decomposition of Δw with respect to the principal stress direction is valid.

Figure 5 shows plots of the decomposed component Δw_y under excitation angles $\varphi_H = \pi/4$ and $\pi/2$. In accordance with principal stress decomposition, the stress dependence along the y -direction is independent of the stress and magnetization along the x -direction. Figure 5 illustrates that the stress along the x -direction slightly affects the iron loss in the y -direction when the magnetization is not large. However, the influence of σ_x increases when B is large. This occurs because the magnetization along the y -direction is not independent from that along the x -direction. Moreover, according to the equivalent stress theory, the compressive stress along the x -direction gives rise to a tensile effect along the y -direction, which makes the influence of σ_x more prominent.

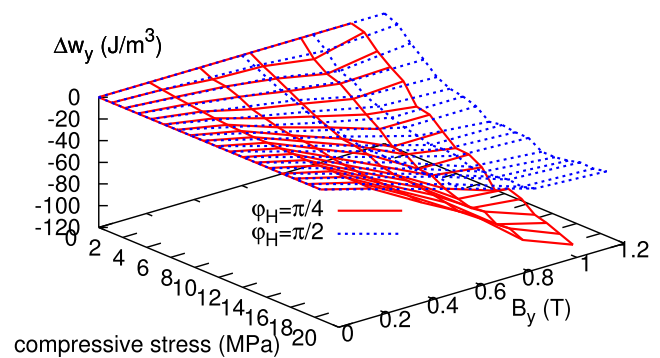


FIG. 5. Comparison of Δw_y when $\varphi_H = \pi/2$ (blue) and $\pi/4$ (red).

V. COMPUTATIONAL TEST

The piezoelectric film used in the experiment can only apply compressive stress on the steel sheet, whereas the measurement under tensile stress has not yet been completed because of the small film size. Furthermore, the applicable range of the compressive

stress was less than 20 MPa under these experimental conditions. A computational test using MDPM was therefore performed to examine the two stress evaluation methods under uniaxial tensile or compressive stress. The material constants required for the computation were as follows: the anisotropy constant for cubic anisotropy was $K = 3.66 \times 10^4 \text{ J/m}^3$, and the magnetostriction constants were $\lambda_{100} = 2.31 \times 10^{-5}$, $\lambda_{111} = -4.3 \times 10^{-6}$, and $\mu_0 M_S = 2.01 \text{ T}$. The pinning distribution is extracted from the measured BH loops under the stress-free condition.

The direction of the applied magnetic field is denoted by φ_H , and the direction of the unidirectional stress is denoted by φ_σ . The magnetization properties along $\varphi = \pi/4$ were simulated using MDPM. Because equivalent stress theory (1) is not valid when the stress is large, a more accurate equivalent stress theory presented in

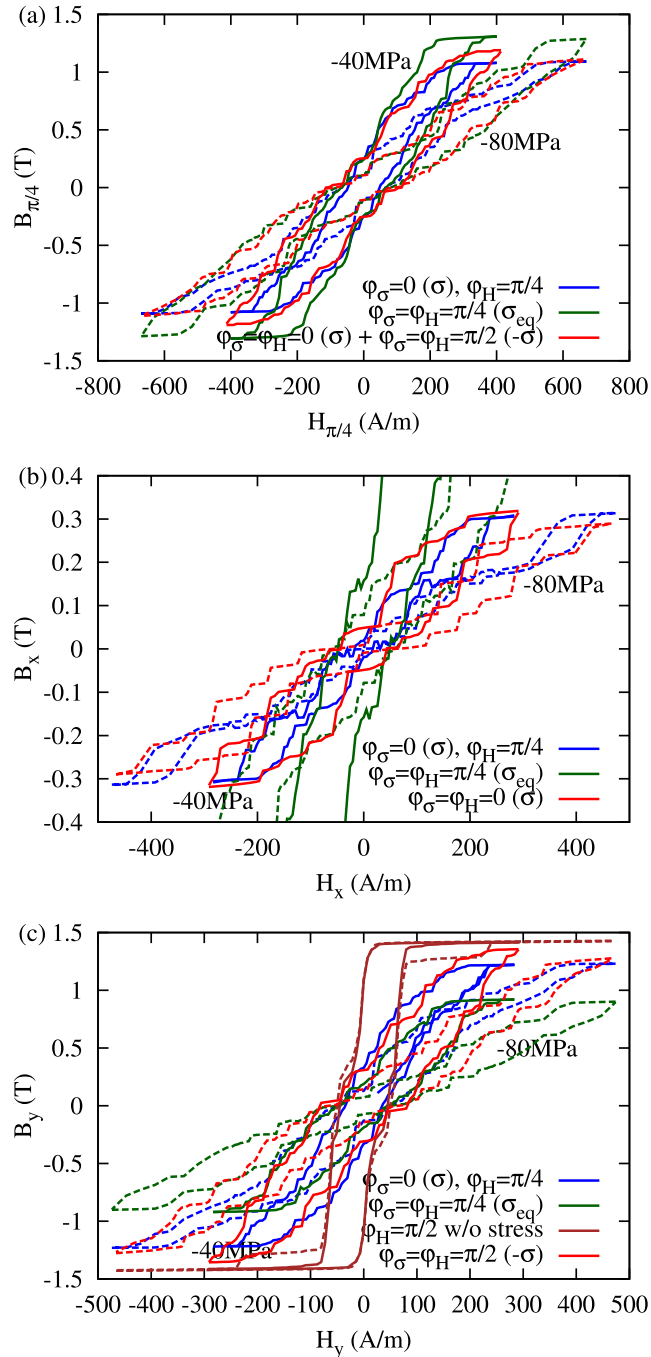


FIG. 6. Simulated BH loops along (a) $\varphi = \pi/4$, (b) $\varphi = 0$, and (c) $\varphi = \pi/2$.

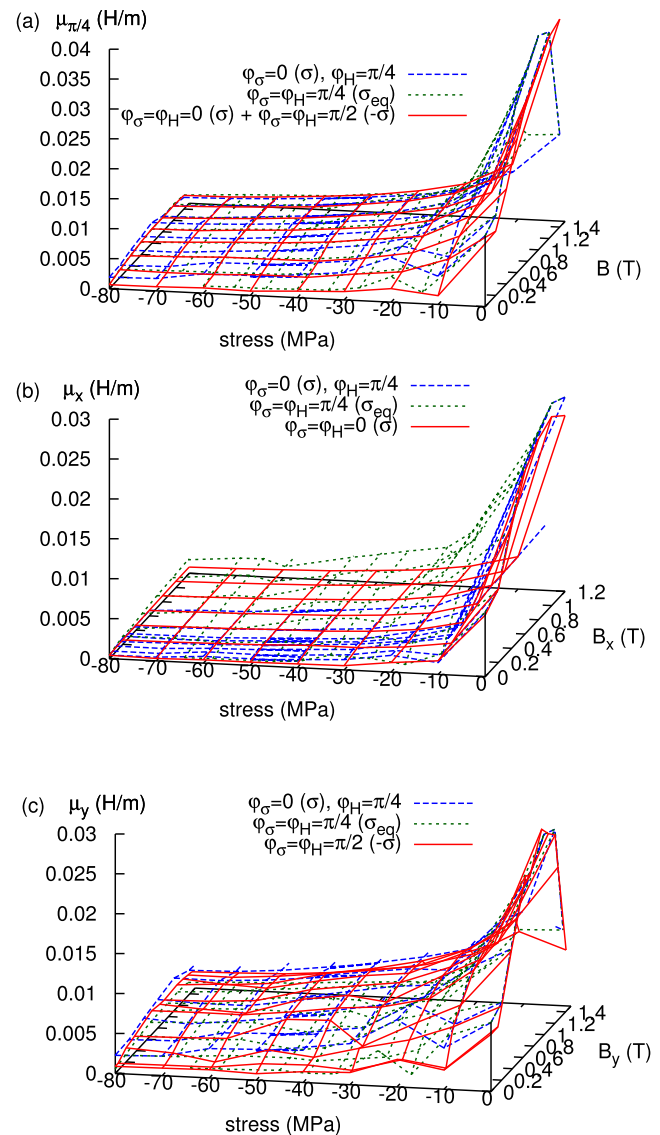


FIG. 7. Simulated average permeability (a) $\varphi = \pi/4$, (b) $\varphi = 0$, and (c) $\varphi = \pi/2$.

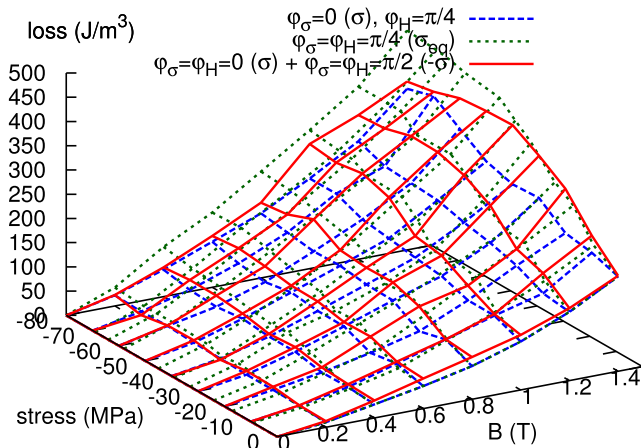


FIG. 8. Simulated hysteresis loss per cycle along $\varphi = \pi/4$.

Ref. 3 is used here, which gives almost the same stress value of Eq. (1) when the stress is small as in Subsection IV A. When a compressive stress of 40 and 80 MPa with $\varphi_\sigma = 0$ is applied, then it appears as if a compressive stress of 13 and 30 MPa is present for $\varphi_\sigma = \pi/4$. Figure 6(a) shows the simulated BH loops along $\varphi = \pi/4$, where the blue lines are loops under compressive stresses of 40 (solid) and 80 (dashed) MPa for $\varphi_\sigma = 0$, whereas the green lines are loops under compressive stresses of 13 and 30 MPa for $\varphi_\sigma = \pi/4$. The equivalent stress theory roughly predicts the stress dependence of BH loops along the excitation direction. Figures 6(b) and 6(c) depict the BH loops decomposed into directions along $\varphi = 0$ and $\pi/2$, where the green lines given by the equivalent stress theory differ from the blue lines primarily because of the incorrect use of the equivalent stress theory.

The red lines in Fig. 6(b) plot the BH loops along $\varphi = 0$ obtained with $\varphi_\sigma = \varphi_H = 0$, where the same compressive stresses of 40 and 80 MPa were applied. The decomposed BH loops were roughly in agreement. The brown lines in Fig. 6(c) plot the BH loops along $\varphi = \pi/2$ obtained with $\varphi_H = \pi/2$ without stress, which fail to predict the decomposed loops. This occurs because the compressive stress along $\varphi = 0$ acts as tensile stress along $\varphi = \pi/2$, as suggested by the equivalent stress theory. The red lines in Fig. 6(c) plot the BH loops obtained with $\varphi_\sigma = \varphi_H = \pi/2$, where tensile stresses of 40 and 80 MPa were applied, which approximately predicted the decomposed loops. The red lines in Fig. 6(a) plot the BH loops synthesized from the decomposed loops, which approximately agree with the loops for $\varphi_H = \pi/4$ (blue lines).

Figure 7 depicts the stress-dependent property of average permeability $\mu_{\pi/4}$, μ_x and μ_y , which are obtained from the computed BH loops with various amplitude along $\varphi = \pi/4$, 0, and $\pi/2$ directions. Figure 8 shows the hysteresis loss per cycle. The same line colors are used as in Fig. 6 to indicate the same computational conditions. The permeability decreases and the loss increases due to the increase in the compressive stress. The equivalent stress theory roughly predicts the magnetic properties along $\varphi = \pi/4$ whereas μ_x is overestimated and μ_y is underestimated. In contrast, the principal stress decomposition method predicts a reasonably accurate stress dependence

when tensile stress is applied in the y -direction. However, an expression for the optimal magnitude of the tensile stress has not been derived theoretically or experimentally, and should be investigated in the future.

VI. CONCLUSION

A principal stress decomposition method was experimentally and computationally examined and compared with the equivalent stress theory. Under unidirectional compressive stress, the principal stress decomposition method provides a reasonable evaluation of the stress-dependent properties in the stress direction; however, it fails to accurately predict the properties in the perpendicular direction. By considering tensile stress in the perpendicular direction, the principal stress decomposition method more accurately predicts the stress dependence of BH loops, permeability and hysteresis loss even when the magnetization direction is different from the stress direction. Accordingly, it is expected that the stress effect on the magnetic properties along different directions from the stress direction can be roughly evaluated by synthesizing the stress-dependent magnetic properties uniaxially measured only along the RD and TD. The stress decomposition under biaxial stress will be discussed in the future.

AUTHOR DECLARATIONS

Conflict of Interest

The authors have no conflicts to disclose.

Author Contributions

H. Shimizu: Investigation (equal); Writing – original draft (equal). **Y. Marumo:** Investigation (equal); Software (supporting). **Y. Mishima:** Investigation (equal); Software (supporting). **T. Matsuo:** Conceptualization (equal); Methodology (equal); Project administration (equal); Software (equal); Supervision (equal); Writing – original draft (equal); Writing – review & editing (equal).

DATA AVAILABILITY

The data supporting the findings of this study are available from the corresponding author upon reasonable request.

REFERENCES

- ¹M. Nakano, C. Fujino, Y. Tani, A. Daikoku, Y. Toide, S. Yamaguchi, H. Arita, and T. Yoshioka, *IEEJ Trans. Ind. Appl.* **129**, 1060 (2009).
- ²O. Hubert and L. Daniel, *J. Magn. Magn. Mater.* **323**, 1766 (2011).
- ³M. Rekik, L. Daniel, and O. Hubert, *IEEE Trans. Magn.* **50**, 2001604 (2014).
- ⁴K. Yamazaki, H. Mukaiyama, and L. Daniel, *IEEE Trans. Magn.* **54**, 1300304 (2018).
- ⁵T. Matsuo, Y. Takahashi, and K. Fujiwara, *J. Magn. Magn. Mater.* **499**, 166303 (2020).
- ⁶H. Kawano, H. Oshima, J. Fujisaki, A. Furuya, Y. Uehara, and T. Matsuo, *IEEE Trans. Magn.* **53**, 8207108 (2017).